DC AND AC CHARACTERISTICS OF ZERO VOLTAGE SWITCHING PWM CONVERTERS

Wisam M. Moussa

IBM Corporation
T78/4-4-392
Endicott, NY 13760

James E. Morris

E.E. Department
SUNY-Binghamton
Binghamton, NY 13902

Zero Voltage Switching (ZVS) can reduce turn-on losses in switching converters, which are the dominant converter power losses at high frequency. Conventional Pulse Width Modulation (PWM) converters can exhibit ZVS by employing a resonant transition interval during the switching time to allow for soft switching. This paper presents an equivalent circuit model for Zero Voltage Switching Resonant Transition (ZVS-RT) converters operating with constant frequency which takes into account the resonant transition interval. The analysis is carried out by relating the terminal currents and voltages, through the definition of switching functions, of the power switches responsible for the zero voltage switching action. An equivalent DC circuit model is generated from these relationships. This model is simple and accurate, and can be used to analyze the DC characteristics of the three basic topologies employing ZVS-RT: buck, boost, and buck-boost. This technique can be extended to improve the small-signal analyses of these converters, also it can be applied to converters using BJT as switching devices to account for the impact of the switching times of the devices.

INTRODUCTION

PWM converters operating with constant switching frequency can reduce switching losses by employing a resonant transition (RT) time to allow for zero voltage switching (ZVS) during the switching interval. This technique can be implemented [1] by replacing both the transistor and diode in the converter with two bidirectional power switches. Each of these switches contains a parallel capacitor and an anti-parallel diode (a MOSFET will suffice with its body diode and input capacitance) as shown in Figure 1. When these converters are modeled as conventional PWM converters, using state-space averaging techniques [2], there is a loss of accuracy caused by ignoring the resonant transition time. This is because state-space averaging representation is inadequate for the prediction of the effects of the intervals between successive modes which appear in these switching converters. There is a need to account for the resonant transition, as it could restrict the switching frequency of the ZVS-RT converter. In what follows, exact steady-state analysis of a ZVS-RT buck converter is carried out where the characteristics of the DC conversion ratio are determined. Following, new models is derived, which takes the resonant transition interval into account. The models are derived through the simple replacement of the switching action in the converter

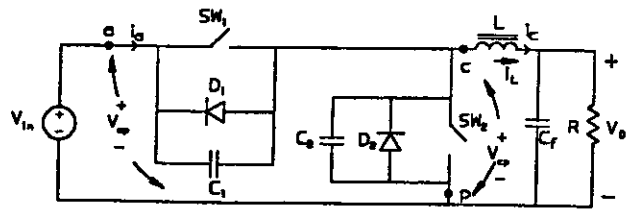

(a) ZVS-RT Buck Converter

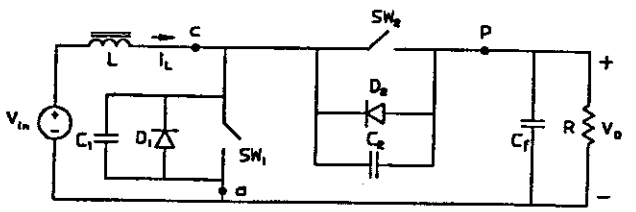

(b) ZVS-RT Boost Converter

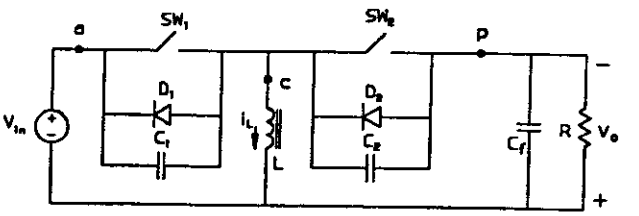

(c) ZVS-RT Buck-Boost Converter

Figure 1. ZVS-RT converters.

by an equivalent linear circuit models. These models can be used for the DC and AC analysis of these converters and is used to derive the DC conversion ratio for the ZVS-RT buck converter. A comparison is made between the exact analysis and the model. A summary table for the three converters is presented.

STEADY STATE ANALYSIS

To simplify the analysis the following assumptions are made: 1) Zero voltage switching is achieved under all operating conditions. 2) Switching devices are assumed to be ideal, i.e., the ON voltage drops across the devices are zero. 3) Capacitors C_1 and C_2

0-7803-0695-3/92 $3.00 © 1992 IEEE

are assumed to be constant and equal $\left[C_1 = C_2 = \frac{C}{2}\right]$. The following analysis corresponds to the operation of the ZVS - RT buck converter. The exact switching waveforms are shown in Figure 2. Assuming the converter has been turned on for a long enough time that it has reached its steady state operating point, and assuming all the transients have died out, a complete switching cycle of the converter will go through four modes of operation. The state equation descriptions of these modes with their initial conditions [4], and the substitution of the operating point at the end of each mode of operation, result in the following system of nonlinear equations, given by:

$$\frac{1-M}{M}\left(1-\cos\alpha_3+\alpha_2\sin\alpha_3-\frac{\cos\alpha_1\sin\alpha_3}{\sin\alpha_1}\right)-\frac{\sin\alpha_3}{\sin\alpha_1}=0 \tag{1}$$

$$\frac{M-1}{M}\left(\frac{1}{\sin\alpha_1}+\alpha_2\cos\alpha_3-\frac{\cos\alpha_1\cos\alpha_3}{\sin\alpha_1}+\sin\alpha_3\right)-\left(\frac{\cos\alpha_1}{\sin\alpha_1}-\frac{\cos\alpha_3}{\sin\alpha_1}\right)+\alpha_4=0 \tag{2}$$

$$\frac{\omega T_s}{Q}+\frac{1-M}{M}\left[\frac{\cos\alpha_1}{\sin\alpha_1}(\alpha_2+\sin\alpha_3+\alpha_4\cos\alpha_3)\right]+\frac{1-M}{M}\left[-\frac{\alpha_2^2}{2}+(1-\alpha_2\alpha_4)\cos\alpha_3-(\alpha_2+\alpha_4)\sin\alpha_3\right]+\frac{1}{\sin\alpha_1}(\alpha_2+\sin\alpha_3+\alpha_4\cos\alpha_3)+\frac{\alpha_4^2}{2}+1=0 \tag{3}$$

$$\omega T_s-\alpha_1-\alpha_2-\alpha_3-\alpha_4=0 \tag{4}$$

where $M=\frac{V_o}{V_{in}}$, $Q=\frac{R}{Z}$, $\omega=1/\sqrt{LC}$, $Z=\sqrt{L/C}$ $\alpha_n=\omega(t_n-t_{n-1})$ and T_s is switching period. Equations (1-4) can be solved numerically for M, the DC conversion ratio of the converter. The solutions are shown in Figure 3, which show the dependence of M on the normalized frequency for a given operating duty ratio and a given load. This is in contrast to the conventional PWM converters, where M is a constant and independent of frequency and load when operating in the continuous conduction mode. In what follows, a new model is derived that represents the behavior of M, which takes into account the transition interval. This will contribute to better accuracy for M than when the resonant transition is ignored.

DEVELOPMENT OF THE MODEL

Assuming the transition intervals are very short, such that the inductor current can be assumed to be constant during this interval, the switching waveforms of the ZVS-RT converters can be approximated as shown in Figure 4, the relationship between instantaneous

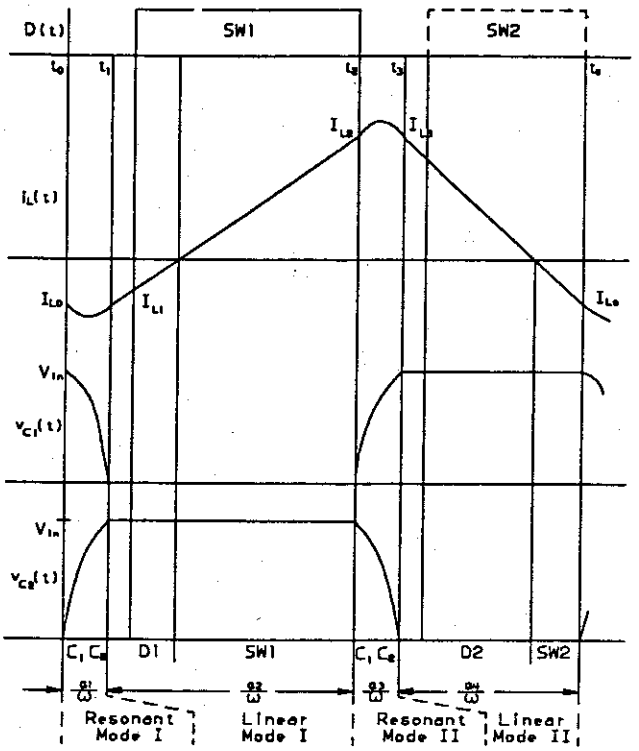

Figure 2. Exact switching waveforms for ZVS-RT buck converter.

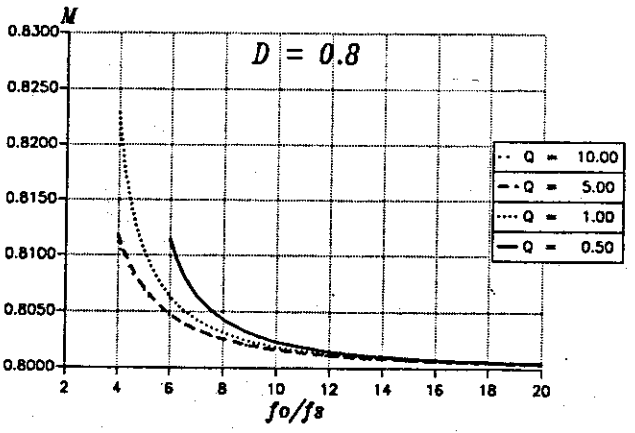

Figure 3. M vs. Normalized frequency for D = 0.8.

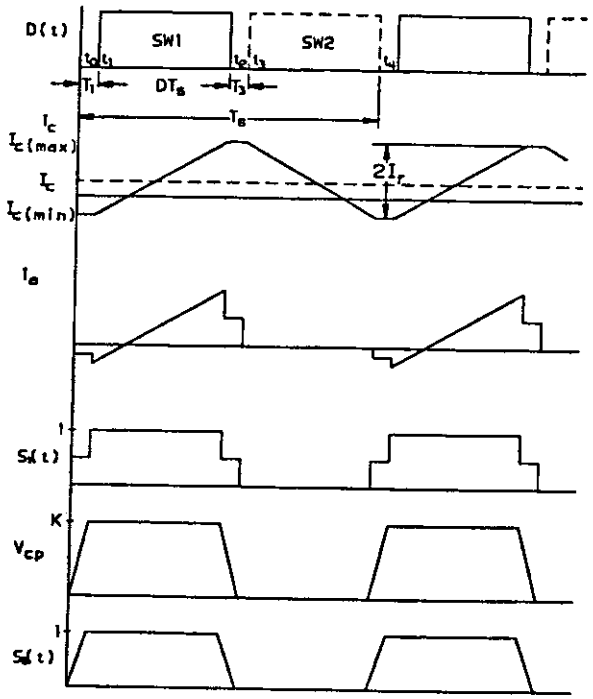

Figure 4. Approximate zero voltage switching waveforms.

terminal currents and terminal voltages can be deduced and shown to be:

$$i_a(t) = s_1(t) i_c(t) \tag{5}$$

and

$$v_{cp}(t) = s_2(t) v_{ap}(t) \tag{6}$$

where $s_1(t)$ and $s_2(t)$ are referred to as the ***switching functions***, as defined in Figure 4, and where K in the figure is a constant that depends on the topology. Equations (5) and (6) constitute a complete description of the model, since Kirchoff's law for current or voltage ensures that the third terminal current or voltage can be expressed in terms of the 2 terminals given in Equations (5) and (6). It is very important to note that the switching functions $s_1(t)$ and $s_2(t)$ include the resonant transition intervals present in the switching circuit.

Averaging

Since the signals of interest are dominated by their averages over the switching period, T_s, therefore Eqs. (5) and (6) can be replaced by their steady-state averaged quantities, given by:

$$\langle i_a(t) \rangle = \frac{1}{T_s} \sum_{i=1}^{4} \int_{t_{i-1}}^{t_i} s_1(t) i_c(t) dt \tag{7}$$

where

$$\sum_{i=1}^{4} t_i - t_{i-1} = T_s \tag{8}$$

Substituting the corresponding values for $i_c(t)$ and $s_1(t)$ for each interval from Figure 4:

$$\langle i_a(t) \rangle = \frac{1}{T_s} \left[I_{c(\min)} \frac{T_1}{2} + \frac{I_{c(\max)} + I_{c(\min)}}{2} DT_s + I_{c(\max)} \frac{T_3}{2} \right] \tag{9}$$

$I_{c(min)}$ and $I_{c(max)}$ are the min/max values of i_c. The two resonant intervals T_1 and T_3, are the minimum blanking times required for the resonant transition intervals to achieve zero voltage switching. Assuming $T_1 \equiv T_3$, they can both be replaced by their average, $\frac{T_1 + T_3}{2}$, hence (9) can be written as:

$$\langle i_a(t) \rangle \simeq \langle s_1(t) \rangle \langle i_c(t) \rangle \tag{10}$$

where

$$\langle i_c(t) \rangle = I_c = \frac{I_{c(\max)} + I_{c(\min)}}{2} \tag{11}$$

and

$$\langle s_1(t) \rangle = S_1(D, I_c, V_{ap}) = D + D_r \tag{12}$$

with D, the duty ratio of modulation, defined as the ratio of the duration of the turn-on pulse, T_{on}, of the PWM signal to the switching period, T_s. f_s is the switching frequency ($f_s = 1/T_s$), D_r is the resonance duty ratio defined as:

$$D_r = \frac{1}{2}(T_1 + T_3) f_s \tag{13}$$

Similarly averaging for (6), assuming small ripple voltage:

$$\langle v_{cp}(t) \rangle \simeq \langle v_{ap}(t) \rangle \langle s_2(t) \rangle \tag{14}$$

where

$$\langle s_2(t) \rangle = S_2(D, I_c, V_{ap}) = D + D_r \tag{15}$$

and

$$\langle v_{ap}(t) \rangle = V_{ap} \tag{16}$$

Noting that I_c is the inductor current, V_{ap} is the voltage impressed upon the switches for the three converters, it is clear that both determine the

resonant transition intervals, which can be written as:

$$T_{1,3} = \left(\frac{CV_{ap}}{I_r \pm I_c} \right) \tag{17}$$

where the positive term refers to T_1. I_r is half the ripple current in the output inductor, given by:

$$I_r = \frac{V_{ac}}{2L} DT_s \tag{18}$$

The ratio I_r/I_c should be greater than 1 to achieve ZVS and for proper operation of the converters. Substituting (17) in (13), D_r can be written as:

$$D_r = \frac{1}{2} \frac{Q^2 D\left(1 - \frac{V_{cp}}{V_{ap}}\right)}{\left[\left(1 - \frac{V_{cp}}{V_{ap}}\right)kD\right]^2 - G_T^2 R^2} \tag{19}$$

where the following definitions are made:

$$G_T = \frac{I_c}{V_{ap}} \quad \text{and} \quad k = \frac{RT_s}{2L} = \pi \frac{f_o}{f_s} Q \ , \tag{20}$$

R is the output load, $f_o = 1/2\pi\sqrt{LC}$ is the resonant frequency, and k is a parameter that determines the critical condition for proper operation to achieve ZVS. This parameter k is similar to the parameter K in [3] for the conventional PWM converter which determines the transition conditions of the modes of operation of the converter from CCM to DCM.

Small-Signal Perturbation and Linearization

The above model undergoes a small perturbation around a steady-state operating point given by:

$$\begin{aligned} v_{cp} &= V_{cp} + \hat{v}_{cp} & i_c &= I_c + \hat{i}_c \\ v_{ap} &= V_{ap} + \hat{v}_{ap} & d &= D + \hat{d} \end{aligned} \tag{21}$$

and:

$$s_j = S_j + \hat{s}_j \qquad j = 1,2 \tag{22}$$

where the variations of s_j are given by:

$$\hat{s}_j \equiv dS_j = \frac{\partial S_j}{\partial D}\hat{d} + \frac{\partial S_j}{\partial I_c}\hat{i}_c + \frac{\partial S_j}{\partial V_{ap}}\hat{v}_{ap} \qquad j = 1,2 \tag{23}$$

where upper case letters represent DC quantities and lower case letters with a hat represent small-signal AC quantities. Assuming the perturbations are small enough such that:

$$\begin{aligned} \frac{\hat{v}_{cp}}{V_{cp}} &<< 1 & \frac{\hat{i}_c}{I_c} &<< 1 \\ \frac{\hat{v}_{ap}}{V_{ap}} &<< 1 & \frac{\hat{d}}{D} &<< 1 \end{aligned} \tag{24}$$

Substituting (21) in Equation (10) results in:

$$(I_a + \hat{i}_a) = \left[S_1(D, I_c, V_{ap}) + \frac{\partial S_1}{\partial D}\hat{d} + \frac{\partial S_1}{\partial I_c}\hat{i}_c + \frac{\partial S_1}{\partial V_{ap}}\hat{v}_{ap} \right](I_c + \hat{i}_c) \tag{25}$$

Expanding (25) and neglecting products of perturbation terms, the DC solution can be extracted and is found to be:

$$I_a = S_1(D, I_c, V_{ap})I_c \tag{26}$$

and an AC solution is given by:

$$\hat{i}_a = S_i\hat{i}_c + I_c\hat{d} + g_i\hat{v}_{ap} \tag{27}$$

where

$$\begin{aligned} S_i &= S_1 + 2CR_T \frac{\beta}{(\beta^2 - 1)^2} f_s \\ &= S_1 + \frac{2D_r}{\beta^2 - 1} \end{aligned} \tag{28}$$

and

$$\begin{aligned} g_i &= C \frac{\beta}{\beta^2 - 1} f_s \\ &= G_T D_r \end{aligned} \tag{29}$$

where G_T is given by (20).

Similarly for Equation (14):

$$(V_{cp} + \hat{v}_{cp}) = \left[S_2(D, I_c, V_{ap}) + \frac{\partial S_2}{\partial D}\hat{d} + \frac{\partial S_2}{\partial I_c}\hat{i}_c + \frac{\partial S_2}{\partial V_{ap}}\hat{v}_{ap} \right](V_{ap} + \hat{v}_{ap}) \tag{30}$$

from which the DC solution is given by:

$$V_{cp} = S_2(D, I_c, V_{ap})V_{ap} \tag{31}$$

and a small-signal AC solution is given by:

$$\hat{v}_{cp} = S_v\hat{v}_{ap} + V_{ap}\hat{d} + r_v\hat{i}_c \tag{32}$$

where the incremental resistance, r_v is given by:

$$\begin{aligned} r_v &= 2CR_T^2 \frac{\beta}{(\beta^2 - 1)^2} f_s \\ &= R_T \frac{2D_r}{\beta^2 - 1} \end{aligned} \tag{33}$$

and

$$\begin{aligned} S_v &= S_2 + CR_T \frac{\beta}{\beta^2 - 1} f_s \\ &= D + 2D_r \end{aligned} \tag{34}$$

From Equations (26) and (31), (27) and (32), DC and AC models are generated and shown in Figure 5. These models can be substituted in the circuit for calculating steady-state and small-signal transfer functions.

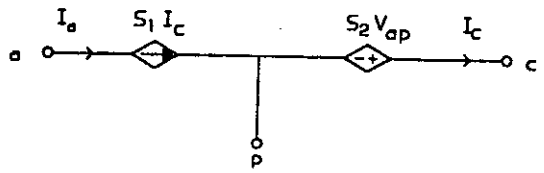

(a) DC model

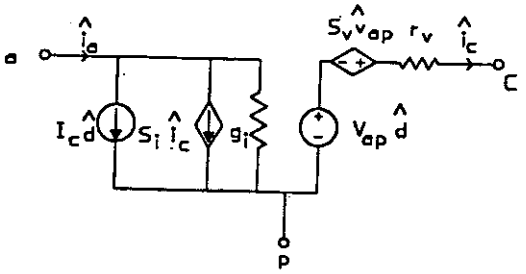

(b) AC model

Figure 5. Equivalent DC and AC models for ZVS-RT converters.

The derived DC and AC models account for the transition interval which improves the model by modifying its elements with elements that account for the transition interval. These elements vanish in the limit as D_r approaches zero (that is, ignoring the transition intervals).

DC ANALYSIS

Figure 6 shows the DC model of a ZVS-RT buck converter incorporating the DC switching function model. To compute the DC voltage conversion ratio, the DC operating point is first determined from the figure as:

$$V_{ap} = V_{in} \text{ and } I_c = I_o \tag{35}$$

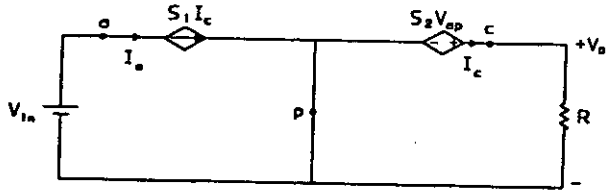

Figure 6. Equivalent DC model for ZVS-RT buck converter.

From Kirchoff's Voltage Law:

$$M = \frac{V_o}{V_{in}} = S_2 = D + D_r \tag{36}$$

where for the buck converter, D_r from (19) is given by:

$$D_r = \frac{1}{2} Q^2 D \frac{(1-M)}{[(1-M)Dk]^2 - M^2} \tag{37}$$

Substituting for D_r in (22):

$$M^3[(Dk)^2 - 1] + M^2[D - (2+D)(Dk)^2] + M\left[(1+2D)(Dk)^2 + \frac{DQ^2}{2}\right] - \left[\frac{DQ^2}{2} + D(Dk)^2\right] = 0 \tag{38}$$

A comparison of M derived from the exact analysis of (1)-(4) and (38) for a given D and Q is shown in Figures 7 and 8. As can be seen from the figures the model gives very good results. The model diverges at lower f_o/f_s, this divergence is attributed to the averaging approximation that took place in deriving the model. The transition times, T_1 and T_3, are closer to their *average* value when the transition interval is small compared to the switching frequency. DC analysis of the three basic converters, buck, boost and buck-boost can be carried out by simply replacing the switching elements in these converters with the *same* DC model shown in Figure 5-a, while maintaining the respective terminals as defined in Figure 1. Table 1 is a summary of the DC transfer characteristics for the three converters. Solutions for the DC conversion ratio for the ZVS-RT boost and buck-boost converters are shown in Figures 9 and 10. It is

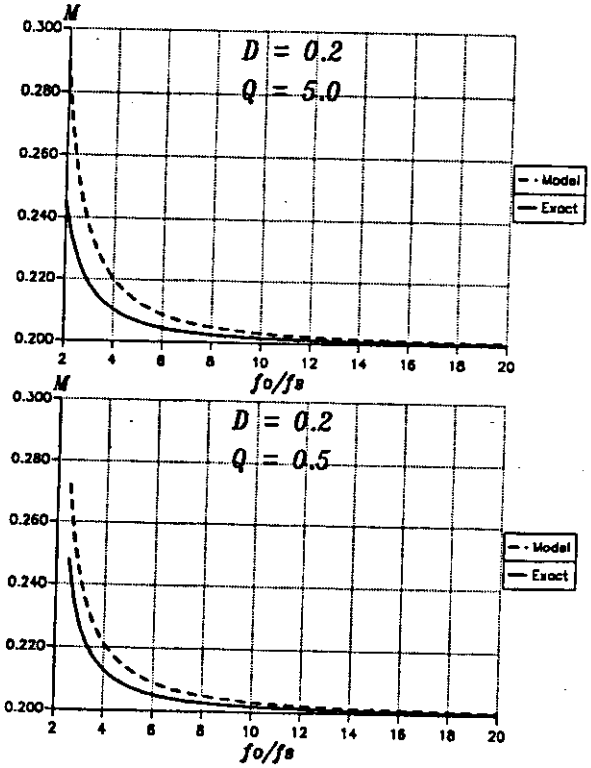

Figure 7. Comparison of M between model and exact analysis.

Table 1. DC transfer functions	
	M
Buck	$M^3\left[(Dk)^2-1\right]+M^2\left[D-(2+D)(Dk)^2\right]+M\left[(1+2D)(Dk)^2+\frac{DQ^2}{2}\right]-\left[\frac{DQ^2}{2}+D(Dk)^2\right]=0$
Boost	$M^5(1-D)-M^4+M^2\frac{DQ^2}{2}+M\left[(D-1)(kD)^2\right]+(kD)^2=0$
Buck-Boost	$M^5(1-D)+M^4(2-3D)+M^3(1-3D)+M^2\left(\frac{DQ^2}{2}-D\right)+M\left[(D-1)(kD)^2+DQ^2\right]+\left[D(kD)^2+\frac{DQ^2}{2}\right]=0$

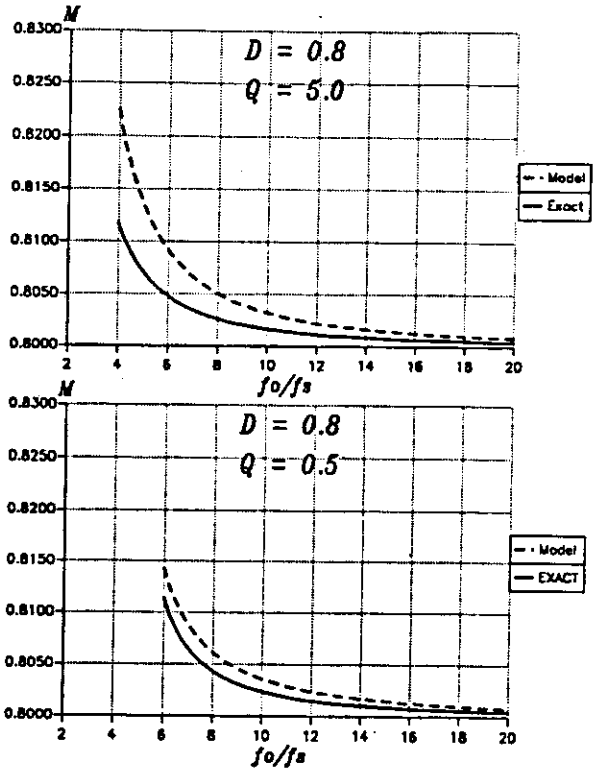

Figure 8. Comparison of M between model and exact analysis.

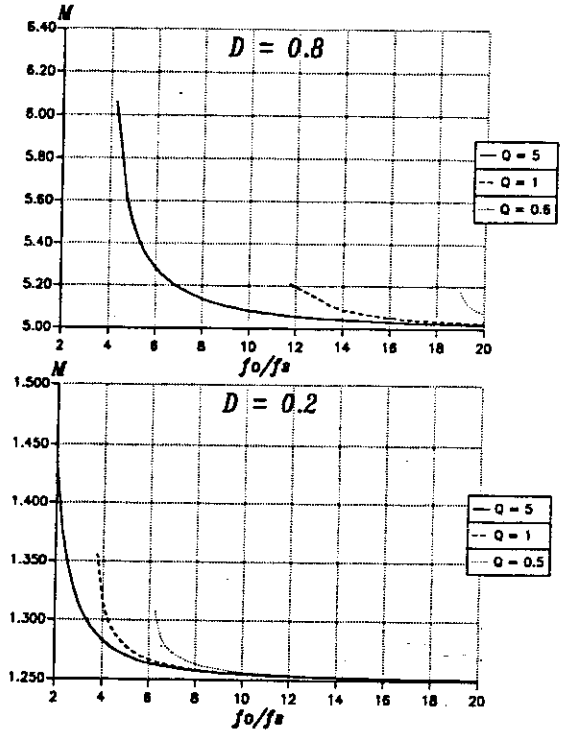

Figure 9. DC conversion ratio for ZVS-RT boost converter.

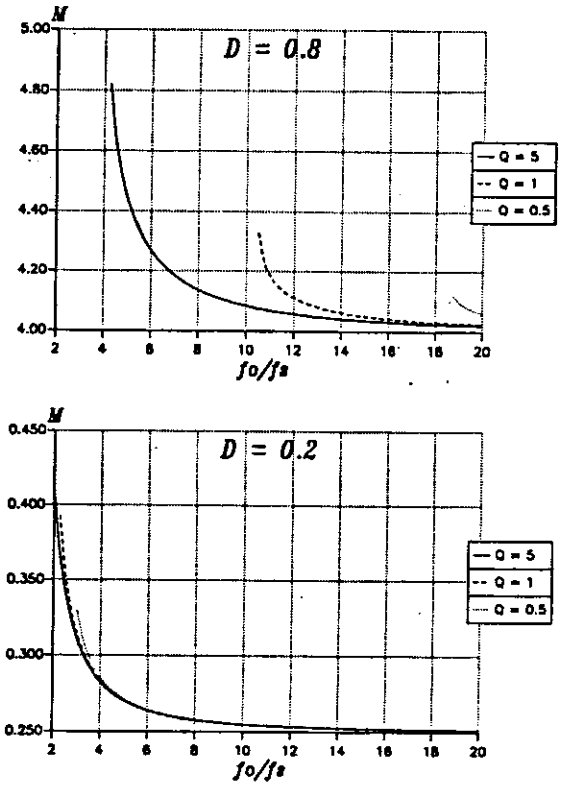

Figure 10. DC conversion ratio for ZVS-RT buck-boost converter.

interesting to note from the figures that the ZVS-RT boost and buck-boost converters that they are more sensitive to the load for high duty cycle than the ZVS-RT buck converter. That is, for a duty cycle of 0.8, a ZVS-RT boost converter operating with a normalized frequency of 12 should have a load current Q > 1.

Similarly, AC analysis can be carried out using the AC model shown in Figure 5-b to determine the AC characteristics fOR the three converters.

CONCLUSIONS

A complete and exact analysis for the DC conversion ratio of ZVS-RT converters using circuit analysis is presented. This resulted in a nonlinear system of equations which were solved numerically. The analysis showed that M depends on the resonant transition interval. A new model for these converters was derived using switching functions that include the resonant transition. This technique leads to simplified analyses and an easy model that can be readily used for simulation. Taking the transition interval into account contributes to better accuracy for the DC conversion ratio M. This model can be used for the DC analysis of these converters. As can be noted from the above analysis, a system of nonlinear equations, which has to be solved numerically with a special purpose program, is reduced here into one of solving the roots of a polynomial which can be found using a simple root finder program. This approach can be extended to derive an equivalent AC small-signal model which can be used to improve the small-signal transfer functions for these converters. Also it can be applied to converters using BJT as switching devices to account for the impact of the switching times [5], where it can be shown that the storage time of the BJT does in fact introduce a modulation resistance in the model.

REFERENCES

[1] C. P. Henze, H. C. Martin and D. W. Parsley, "Zero-Voltage Switching in High Frequency Power Converters Using Pulse Width Modulation," IEEE APEC Conf. Rec., pp. 33-40, 1988.

[2] R. D. Middlebrook and S. C'uk, "A General Unified Approach to Modelling Switching Converters in Discontinuous Conduction Mode," IEEE PESC Conf. Rec. 1977.

[3] V. Vorperian, "Simplified Analysis of PWM Converter Using the Model of the PWM Switch," IEEE Trans. on AES Vol. 26, No. 3, May 1990.

[4] V. Vorperian, "Quasi-Square Wave Converters: Topologies and Analysis," IEEE Trans. on Power Electronics Vol. PE-3, No. 2, pp. 183-191, April 1988.

[5] W. Moussa and J. Morris, "Effects of Non-ideal Switches in PWM Switching Converters," International Journal of Electronics, Vol. 72, No. 2, 213-222, February 1992.